

## Enhanced electron screening in d(d,p)t for deuterated metals

C. ROLFS for LUNA collaboration

*Institut für Physik mit Ionenstrahlen, Ruhr-Universität Bochum, Germany*

electron screening effect in the d(d,p)t reaction has been studied for deuterated metals, insulators, and semiconductors, i.e. 58 samples in total. As compared to measurements performed with a gaseous D<sub>2</sub> target, a large effect has been observed in most metals, while a small (gaseous) effect is found e.g. for the insulators, semiconductors, and lanthanides. The periodic table provides the ordering of the observed small and large effects in the samples. An explanation of the large effects in metals is possibly provided by the classical plasma screening of Debye applied to the quasi-free metallic electrons. The data also provide information on the solubility of hydrogen in the samples.

### §1. Introduction

It is well known that the cross section  $\sigma(E)$  of a charged-particle-induced nuclear reaction is enhanced at low energies by the electron clouds surrounding the interacting nuclides, with an enhancement factor<sup>1)</sup>

$$f_{\text{lab}}(E) = E(E + U_e)^{-1} \exp(-2\pi\eta(E + U_e) + 2\pi\eta(E)), \quad \text{for } S(E + U_e) \approx S(E) \quad (1.1)$$

where  $\eta(E)$  is the Sommerfeld parameter,  $S(E)$  the astrophysical S-factor, and  $U_e$  the screening potential energy.

The screening effect in d(d,p)t has been studied previously for 6 deuterated metals,<sup>2),3)</sup> where the resulting  $S(E)$  data showed for 4 metals an exponential enhancement according to equation (2). However, the extracted  $U_e$  values were about one order of magnitude larger than the value found in a gas-target experiment:  $U_e = 25$  eV.<sup>4)</sup> Our study of deuterated Ta led to  $U_e = 340 \pm 14$  eV<sup>5),6)</sup> confirming the previous observation. Recently, we reported on preliminary results for several metals, insulators, and semiconductors.<sup>6),7)</sup> The present report completes these investigations superseding the preliminary results.

### §2. Experimental procedures

The equipment, procedures, and data analysis have been described elsewhere.<sup>5)-7)</sup> The deduced thin-target yield curve,  $Y(E_d, q)$ , is related to the cross section  $\sigma(E_{\text{eff}})$  via

$$Y(E_d, q) = \alpha \epsilon_{\text{eff}}(E_d)^{-1} \sigma(E_{\text{eff}}), \quad (2.1)$$

with the effective energy  $E_{\text{eff}}$  and the constant  $\alpha$ , as measured using a radioactive source. The effective stopping power  $\epsilon_{\text{eff}}(E_d)$  for the deuterated M<sub>x</sub>D target is given by the expression

$$\epsilon_{\text{eff}}(E_d) = \epsilon_D(E_d) + x\epsilon_M(E_d). \quad (2.2)$$

Rutherford-Backscattering-Spectrometry of the samples exhibited no detectable surface contamination except for Al which revealed an  $\text{Al}_2\text{O}_3$  surface layer with a thickness of about 150 monolayers. Since this thickness is larger than the energy step in our differentiation method,<sup>5)</sup> the reported  $U_e \leq 30$  eV value<sup>6)</sup> corresponded to the case of an  $\text{Al}_2\text{O}_3$  insulator and not to an Al metal (Table 1). Since Al oxides rapidly in air, we cleaned the Al surface *in situ* by Kr sputtering at 15 keV (at the 100 kV accelerator) removing at least 100 monolayers. After this cleaning the experimental procedure<sup>5)</sup> was carried out leading to  $U_e = 520 \pm 50$  eV for the metal Al (Table I). This surface cleaning by Kr sputtering was carried out subsequently as a first step in the experimental procedures, for each new sample as well as for all of the previously studied samples,<sup>6),7)</sup> where the target temperature was always  $T = 20$  °C; in particular, the noble metals Cu, Ag, and Au exhibited - after this cleaning procedure - also a large enhancement effect.

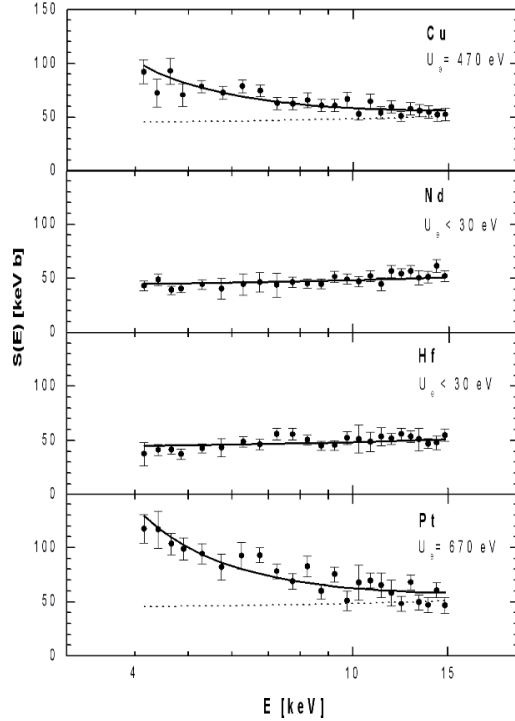


Fig. 1. Astrophysical  $S(E)$  factor of the reaction  $d(d,p)t$  as obtained for the deuterated samples Cu, Nd, Hf, and Pt ( $E$  = effective center-of-mass energy). The dotted curve represents the bare  $S(E)$  factor, while the solid curve includes the exponential enhancement due to electron screening with the  $U_e$  value given.

The resulting cross section  $\sigma(E_{\text{eff}})$  is illustrated in Fig. 1 in form of the astrophysical  $S(E)$  factor for the examples Cu, Nd, Hf, and Pt. The absolute scale was obtained by normalisation to previous work<sup>4)</sup> at  $E_d = 30$  keV including the effects of electron screening where applicable. The normalisation led to a value for the stoichiometric ratio  $x$  given in Table I in form of the hydrogen solubility  $1/x$ .

In the analysis of the data (e.g. Fig. 1) we assumed a bare  $S(E)$  factor (i.e.

Table I. Summary of results <sup>a</sup>

	$U_e$ (eV) <sup>b</sup>	$1/x$ <sup>c</sup>	$n_{\text{eff}}$ <sup>b</sup>	$n_{\text{eff}}(\text{Hall})$ <sup>d</sup>		$U_e$ (eV) <sup>b</sup>	$1/x$ <sup>c</sup>
<b>metals</b>					<b>semiconductors</b>		
Be	180 ± 40	0.08	0.2 ± 0.1	(0.21 ± 0.04)	C	≤ 60	0.35
Mg	440 ± 40	0.11	3.0 ± 0.5	1.8 ± 0.4	Si	≤ 60	0.23
Al	520 ± 50	0.26	3.0 ± 0.6	3.1 ± 0.6	Ge	≤ 80	0.56
V	480 ± 60	0.04	2.1 ± 0.5	(1.1 ± 0.2)	<b>insulators</b>		
Cr	320 ± 70	0.15	0.8 ± 0.4	(0.20 ± 0.04)	BeO	≤ 30	0.25
Mn	390 ± 50	0.12	1.2 ± 0.3	(0.8 ± 0.2)	B	≤ 30	0.38
Fe	460 ± 60	0.06	1.7 ± 0.4	(3.0 ± 0.6)	Al <sub>2</sub> O <sub>3</sub>	≤ 30	0.27
Co	640 ± 70	0.14	3.1 ± 0.7	(1.7 ± 0.3)	CaO <sub>2</sub>	≤ 50	0.60
Ni	380 ± 40	0.13	1.1 ± 0.2	1.1 ± 0.2	<b>groups 3 and 4</b>		
Cu	470 ± 50	0.09	1.8 ± 0.4	1.5 ± 0.3	Sc	≤ 30	1.4
Zn	480 ± 50	0.13	2.4 ± 0.5	(1.5 ± 0.3)	Ti	≤ 30	1.3
Sr	210 ± 30	0.27	1.7 ± 0.5		Y	≤ 70	1.8
Nb	470 ± 60	0.13	2.7 ± 0.7	(1.3 ± 0.3)	Zr	≤ 40	1.1
Mo	420 ± 50	0.12	1.9 ± 0.5	(0.8 ± 0.2)	Lu	≤ 40	1.5
Ru	215 ± 30	0.18	0.4 ± 0.1	(0.4 ± 0.1)	Hf	≤ 30	1.8
Rh	230 ± 40	0.09	0.5 ± 0.2	(1.7 ± 0.4)	<b>lanthanides</b>		
Pd	800 ± 90	0.03	6.3 ± 1.3	1.1 ± 0.2	La	≤ 60	0.6
Ag	330 ± 40	0.14	1.3 ± 0.3	1.2 ± 0.3	Ce	≤ 30	1.3
Cd	360 ± 40	0.18	1.9 ± 0.4	(2.5 ± 0.5)	Pr	≤ 70	0.9
In	520 ± 50	0.02	4.8 ± 0.9		Nd	≤ 30	0.7
Sn	130 ± 20	0.08	0.3 ± 0.1		Sm	≤ 30	1.3
Sb	720 ± 70	0.13	11 ± 2		Eu	≤ 50	0.6
Ba	490 ± 70	0.21	9.9 ± 2.9		Gd	≤ 50	1.4
Ta	270 ± 30	0.13	0.9 ± 0.2	(1.1 ± 0.2)	Tb	≤ 30	1.3
W	250 ± 30	0.29	0.7 ± 0.2	(0.8 ± 0.2)	Dy	≤ 30	1.1
Re	230 ± 30	0.14	0.5 ± 0.1	(0.3 ± 0.1)	Ho	≤ 70	1.6
Ir	200 ± 40	0.23	0.4 ± 0.2	(2.2 ± 0.5)	Er	≤ 50	1.0
Pt	670 ± 50	0.06	4.6 ± 0.7	3.9 ± 0.8	Tm	≤ 70	1.4
Au	280 ± 50	0.18	0.9 ± 0.3	1.5 ± 0.3	Yb	≤ 40	1.3
Tl	550 ± 90	0.01	5.8 ± 1.2	(7.4 ± 1.5)			
Pb	480 ± 50	0.04	4.3 ± 0.9				
Bi	540 ± 60	0.12	6.9 ± 1.5				

<sup>a</sup> For a target temperature of  $T = 20$  °C and a surface cleaning by Kr sputtering

<sup>b</sup> Error contains no systematic uncertainty in stopping power

<sup>c</sup> Estimated uncertainty is about 20%

<sup>d</sup> From the observed Hall coefficient at  $T = 20$  °C, with an assumed 20% error; the numbers in brackets are for hole carriers

for bare interacting nuclides) linearly increasing with energy,  $S_b(E) = 43 + 0.54E$  [keV b] (center-of-mass energy  $E$  in keV), as found previously.<sup>4),5)</sup> Relative to this function, the data were fitted with the enhancement factor of equation : the resulting  $U_e$  values are summarized in Table I. In one experiment, we increased the target temperature to  $T = 100$  °C using diffilen oil supplied by a cryo-circulator (JULABO FP90), whereby a thermoelement had been placed behind the target to measure  $T$  with a precision of 2 °C (including beam-heating effects). For deuterated Pt we find  $U_e = 530 \pm 40$  eV (with  $1/x = 0.06$ ) showing a decrease of  $U_e$  with increasing  $T$  (for



equation 1, the enhanced cross section is most likely due to electron effects of the environment of the target deuterons. Various aspects of the metals were discussed previously to explain possibly the data:<sup>5),6)</sup> stopping power, thermal motion, channeling, diffusion, conductivity, crystal structure, electron configuration, and “Fermi shuttle” acceleration mechanism; however, none of these aspects led to a solution.

If  $n_{\text{eff}}$  is the number of valence electrons per metallic atom which can be effectively treated as classical and quasi-free, one may apply the classical plasma theory of Debye leading to an electron sphere of radius<sup>9)</sup>

$$R_D = (\epsilon_0 kT / e^2 n_{\text{eff}} \rho_a)^{1/2} = 69(T / n_{\text{eff}} \rho_a)^{1/2} \quad [\text{m}] \quad (3.1)$$

around positive singly-charged ions (here: deuterons in the lattice) with the temperature of the free electrons  $T$  in units of K and the atomic density  $\rho_a$  in units of  $\text{m}^{-3}$ . For  $T = 293$  K,  $\rho_a = 6 \times 10^{28} \text{ m}^{-3}$ , and  $n_{\text{eff}} = 1$  one obtains a radius  $R_D$ , which is about a factor 10 smaller than the Bohr radius of a hydrogen atom. With the Coulomb energy between two deuterons at  $R_D$  set equal to  $U_e$ , one obtains  $U_e = (4\pi\epsilon_0)^{-1} e^2 / R_D = 300$  eV, the order of magnitude of the observed  $U_e$  values. A comparison of the calculated and observed  $U_e$  values leads to  $n_{\text{eff}}$  given in Table I: for most metals  $n_{\text{eff}}$  is of the order of one. The acceleration mechanisms of the incident ions leading to the high observed  $U_e$  values is thus — within our simple model — the Debye electron cloud at the rather small radius  $R_D$ .

A critical test of the classical Debye model is the predicted temperature dependence,  $U_e \propto T^{-1/2}$ . For deuterated Pt we find a ratio  $R_{\text{exp}} = U_e(100^\circ\text{C}) / U_e(20^\circ\text{C}) = 0.79 \pm 0.08$ , in fair agreement with the expected value  $R_{\text{theo}} = 0.88 \pm 0.01$  from our model. If one includes the observed  $8 \pm 2\%$  decrease of  $n_{\text{eff}}$  over this temperature range (see below), the agreement is somewhat better ( $R_{\text{theo}} = 0.84 \pm 0.02$ ). A new setup is in preparation to extend the measurements to significantly higher temperatures (more than  $400^\circ\text{C}$ ). It has been found that at low temperatures the hydrogen solubility increases rapidly such that the material becomes an insulator (e.g. Ta as reported in 5)).

An alternative determination of  $n_{\text{eff}}$  is obtained from the observed Hall coefficient for metals at room temperature (10) and references therein),

$$C_{\text{Hall}} = (en_{\text{eff}}(\text{Hall})\rho_a)^{-1}, \quad (3.2)$$

where for about 50% of the metals in Table I the coefficient is negative (electron carriers) and for the other one-half it is positive (hole carriers). Since in the latter case essentially also electrons move (however in the opposite direction), we assumed that any dependence on the + or – sign of  $C_{\text{Hall}}$  can be neglected (which needs theoretical verification). The resulting  $n_{\text{eff}}(\text{Hall})$  values are also given in Table I: there is a remarkable correlation between  $n_{\text{eff}}$  and  $n_{\text{eff}}(\text{Hall})$  both for electron and hole carriers, i.e. within 2 standard deviations the two quantities agree for all metals with a known Hall coefficient, except for Pd and Ir. Our own measurement of the Hall coefficient for Pd led to  $n_{\text{eff}}(\text{Hall}) = 3.4 \pm 0.7$  removing essentially the discrepancy with  $n_{\text{eff}} = 6.3 \pm 1.3$ . Thus, it appears desirable to measure or remeasure the Hall coefficient for all metals with a high  $U_e$  value (Table I).

Although the classical Debye model appears to explain to a large extent the data, it is well known that most of the conduction electrons are not classical but are frozen by quantum effects and only electrons close to the Fermi energy ( $E_F$ ) actually should contribute to screening. A standard calculation of a Fermi gas at low temperature ( $kT \ll E_F$ ) yields an effective number  $n_{\text{eff}}(\text{Fermi}) = 0.67kT/E_F$  and correspondingly the screening potential energy  $U_e$  should be about 10 eV at room temperature (for  $E_F = 3$  eV). However, near room temperature the Hall coefficient  $C_{\text{Hall}}$  is observed for many metals to increase with temperature,<sup>10)</sup> e.g. for Pt by 8% between  $T = 20$  °C and 100 °C, while from  $n_{\text{eff}}(\text{Fermi})$  one expects a decrease for  $C_{\text{Hall}}$  by 34% over this temperature range. Furthermore, inserting  $n_{\text{eff}}(\text{Fermi})$  into equation (3.1), one expects no temperature dependence for  $U_e$ , in conflict with our observation. Thus, the data for the electron screening as well as for the Hall coefficient suggest some deviation from this simple however well established treatment of conduction electrons.

It should be pointed out finally that improved measurements of the electron screening effects in deuterated materials require an Ultra-High-Vacuum system with in situ analysis methods of high depth resolution such as SIMS, AES and XPS to characterize in deeper detail the environment of the deuterium atoms at the surface.

#### References

- 1) H.J.Assenbaum, K.Langanke, C.Rolfs: Z. Phys. A327(1987)461
- 2) K.Czerski et al.: Europhys. Lett. 54(2001)449
- 3) H.Yuki et al.: JETP Lett. 68(1998)823
- 4) Ue.Grife et al.: Z. Phys. A351(1995)107
- 5) F.Raiola et al.: Eur. Phys. J. A13(2002)377
- 6) F.Raiola et al.: Phys.Lett. B547(2002)193
- 7) C.Bonomo et al.: Nucl.Phys. A719(2003)37c
- 8) W.M.Mueller, J.P.Blackedge, G.G.Libowitz: Metal Hydrides (Academic Press, New York, 1968); F.A.Lewis, A.Aladjem: Hydrogen Metal Systems (Solid State Phenomena, Vol. 49-50, Scitec Publ., Zürich, 1996)
- 9) F.F.Chen: Introduction to plasma physics and controlled fusion (Plenum, New York, 1984)
- 10) Landolt-Börnstein, Vol. II.6 (Springer, Berlin, 1959); C.M.Hurd: The Hall effect in metals and alloys (Plenum Press, 1972)